

Potato CYCLING DOF FACTOR 1 and its lncRNA counterpart *StFLORE* link tuber development and drought response

Lorena Ramírez Gonzales¹, Li Shi¹, Sara Bergonzi Bergonzi¹ , Marian Oortwijn¹, José M. Franco-Zorrilla³ , Roberto Solano-Tavira³ , Richard G. F. Visser¹ , José A. Abelenda^{2,†} , and Christian W. B. Bachem^{1,*,†} 

¹Plant Breeding, Wageningen University & Research, PO Box 386, Wageningen 6700 AJ, the Netherlands,

²Centro de Biotecnología y Genómica de Plantas, Universidad Politécnica de Madrid (UPM), Instituto Nacional de Investigación y Tecnología Agraria y Alimentaria (INIA), Madrid 28040, Spain, and

³Departamento de Genética Molecular de Plantas, Centro Nacional de Biotecnología – CSIC, Madrid 28049, Spain

Received 6 May 2020; accepted 9 November 2020; published online 21 November 2020.

*For correspondence (e-mail christian.bachem@wur.nl).

†These authors contributed equally to this work.

SUMMARY

Plants regulate their reproductive cycles under the influence of environmental cues, such as day length, temperature and water availability. In *Solanum tuberosum* (potato), vegetative reproduction via tuberization is known to be regulated by photoperiod, in a very similar way to flowering. The central clock output transcription factor CYCLING DOF FACTOR 1 (*StCDF1*) was shown to regulate tuberization. We now show that *StCDF1*, together with a long non-coding RNA (lncRNA) counterpart, named *StFLORE*, also regulates water loss through affecting stomatal growth and diurnal opening. Both natural and CRISPR-Cas9 mutations in the *StFLORE* transcript produce plants with increased sensitivity to water-limiting conditions. Conversely, elevated expression of *StFLORE*, both by the overexpression of *StFLORE* or by the downregulation of *StCDF1*, results in an increased tolerance to drought through reducing water loss. Although *StFLORE* appears to act as a natural antisense transcript, it is in turn regulated by the *StCDF1* transcription factor. We further show that *StCDF1* is a non-redundant regulator of tuberization that affects the expression of two other members of the potato *StCDF* gene family, as well as *StCO* genes, through binding to a canonical sequence motif. Taken together, we demonstrate that the *StCDF1–StFLORE* locus is important for vegetative reproduction and water homeostasis, both of which are important traits for potato plant breeding.

Keywords: *Solanum tuberosum*, CYCLING DOF FACTOR, drought tolerance, lncRNA, potato tuberization, stomata, water loss rate.

Linked article: This paper is the subject of a Research Highlight article. To view this Research Highlight article visit <https://doi.org/10.1111/tpj.15175>

INTRODUCTION

Solanum tuberosum L. (potato) is one of the most important non-grain food crops in the world, with increasing importance for the growing economies of India and China. Potato originated in the equatorial Andean region of South America (Spooner *et al.*, 2007), where it tuberizes in response to a short-day (SD) photoperiod. During domestication, the potato crop has also adapted to the long-day photoperiod in the northern latitudes of North America, Europe and Asia (Gutaker *et al.*, 2019). The molecular regulation of tuberization is well understood and bears a striking similarity to the regulation of flowering in most angiosperms (Abelenda *et al.*, 2014).

In *Arabidopsis thaliana*, flowering is regulated by an integrated light- and clock-dependent signalling cascade that includes proteins such as GIGANTEA (GI) and FLAVIN-

BINDING KELCH REPEAT F-BOX 1 (FKF1), which together bind to the carboxyl terminus of CYCLING DOF FACTORS (CDFs), targeting them for degradation (Imaizumi *et al.*, 2005; Sawa *et al.*, 2007). Arabidopsis CDFs act redundantly on the *CONSTANS* (*CO*) promoter, which in turn is an inducer of the florigen, *FLOWERING LOCUS T* (*FT*) (Andres and Coupland, 2012). CDF proteins belong to a larger group of DNA-BINDING WITH ONE FINGER (DOF) transcription factors that bind to a consensus motif in promoters of their target genes (Yanagisawa and Schmidt, 1999; Plesch *et al.*, 2001). Multiple tandem repeats of this motif are also present in the *CO* promoter, and AtCDF1 protein can repress *CO* by binding to these motifs (Imaizumi *et al.*, 2005; Imaizumi and Kay, 2006).

In potato, allelic variation in the 3' of the *StCDF1* gene can lead to a truncation of the coding region, thereby

eliminating the StFKF1 binding site in the protein. The resulting lack of StFKF1-mediated ubiquitination, and subsequent degradation by the proteasome, allows the StCDF1 protein to evade normal diurnal degradation (Kloosterman *et al.*, 2013). This transposon insertion-mediated truncation results in the indirect induction of tuberization through the constitutive repression of *StCO* and *StSP5G* genes, which together repress the transcription of the tuberigen *StSP6A* (Kloosterman *et al.*, 2013; Abelenda *et al.*, 2016). Potato plants carrying one or more of these truncated allelic variants (*StCDF1.2* and *StCDF1.3*) become 'early' and long-day adapted, whereas potato genotypes with the full-length wild-type protein (*StCDF1.1*) are generally 'late', and are therefore SD dependent for tuberization (Kloosterman *et al.*, 2013).

Beyond the regulation of flowering, CDF transcription factors have been associated with abiotic stress tolerance. Overexpression of *Solanum lycopersicum* (tomato) *SICDF1* and *SICDF3* genes in *Arabidopsis* leads to higher tolerance to drought stress and salt stress (Corrales *et al.*, 2014). Furthermore, mutations in *CDF3* of *Arabidopsis* results in increased sensitivity to both drought and low temperatures, whereas increased expression enhances tolerance to drought, cold and osmotic stress (Corrales *et al.*, 2017). A further level of complexity is added to this gene family by the finding that some *CDF* genes also encode a divergently transcribed long non-coding RNA (lncRNA; Ariel *et al.*, 2015) that appears to act as a natural antisense transcript (NAT), regulating *CDF* transcription (Henriques *et al.*, 2017).

Here, we further characterize the molecular mechanisms by which the *StCDF1* locus regulates tuberization and impacts on drought tolerance in potato. We show that StCDF1 strongly binds to the DOF consensus sequence present in the promoters of *StCO1*, *StCO2* and *StCO3* genes. We also demonstrate that although CDFs in *Arabidopsis* show functional redundancy for the regulation of flowering, StCDF1 in potato has a non-redundant role for tuberization. In addition, we find that *StCDF1* has its own natural antisense transcript (*StFLORE*) with antiphasic gene expression over the circadian cycle. Finally, we show that changing *StFLORE* expression has powerful effects on water homeostasis in plants, and that this response is due to the regulation of stomatal opening in an ABA-dependent manner.

RESULTS

StCDF1 binds to the promoter of potato *CONSTANS* genes

We have previously demonstrated that StCDF1 regulates the transcription of *StCO* genes in potato (Kloosterman *et al.*, 2013). To gain more understanding about the sequences that the StCDF1 protein binds to, we used a protein binding microarray (PBM) to identify the consensus

binding sequence for this transcription factor (Godoy *et al.*, 2011; Franco-Zorrilla *et al.*, 2014). For this, the *StCDF1* coding region was cloned in a translational fusion to a maltose binding domain and expressed in *Escherichia coli*, from which protein was extracted and incubated on the PBM. Results from this experiment clearly confirmed the sequence specificity of the StCDF1 protein for the core DOF motif: AAAG (Figure 1a). We were also able to define a wider sequence consensus represented by a 9-bp sequence YWAAAGRYC motif (Figure 1b). Individual nucleotide deviations from the consensus dramatically reduce the specificity of the binding (Figure 1c). Additionally, in a genome-wide scan for the presence of the canonical StCDF1 cognate using the entire upstream region (−1.5 kb) of the annotated genes of the DM1-3 516 R44 (DM) reference genome (Potato Genome Sequencing Consortium, PGSC, 2011), the best-fit curve shows that the most abundant location of the DOF motif is relatively close to the transcriptional start site (Figure 1d) (Franco-Zorrilla *et al.*, 2014). This finding adds biological weight to the determination of the sequence motif (Figure 1c).

We have shown previously that StCDF1 transcriptionally targets *StCO1* and *StCO2* (Kloosterman *et al.*, 2013). Here, we identify an unannotated homolog *StCO3* that is also regulated by circadian rhythm, with a peak during the night (Figure S1a). The three *StCO* genes are in a tandem repeat at chromosome 2 in potato. Using chromatin immunoprecipitation (ChIP) quantitative polymerase chain reaction (qPCR), we demonstrated the direct binding of StCDF1 to the DOF motifs present in the promoters of *StCO* genes *in vivo* (Figure 1e). These experiments clearly show a strong binding and specificity to the promoter region of the *StCO1*, weak binding to the *StCO2* promoter and high relative levels of enrichment in the *StCO3* promoter in the wild-type *Solanum tuberosum* group *Andigenum* background. Another amplified control region of the genome used as a negative control (Actin) shows no binding. The *StCO3* gene is repressed in *35S:StCDF1.2* overexpression lines (Figure S1b), confirming transcriptional regulation by StCDF1. Similarly, it was previously shown that *StCO1* and *StCO2* were also repressed in *35S:StCDF1.2* overexpression lines (Kloosterman *et al.*, 2013). Strikingly, we observed differences between *35S:StCDF1.2* and wild-type (WT) backgrounds in the *StCO3* promoter, probably indicating some type of negative transcriptional regulation of *StCDF1* by itself in the overexpression lines. Taken together, from the ChIP-qPCR and the expression studies in transgenic lines, we conclude that StCDF1 is likely to regulate all of the *StCOs*, with *StCO1* and *StCO3* promoters being the targets with the highest affinity.

StCDF1 is a non-redundant regulator of tuberization

We have previously shown that the overexpression of *StCDF1.2* strongly promotes tuberization in potato and

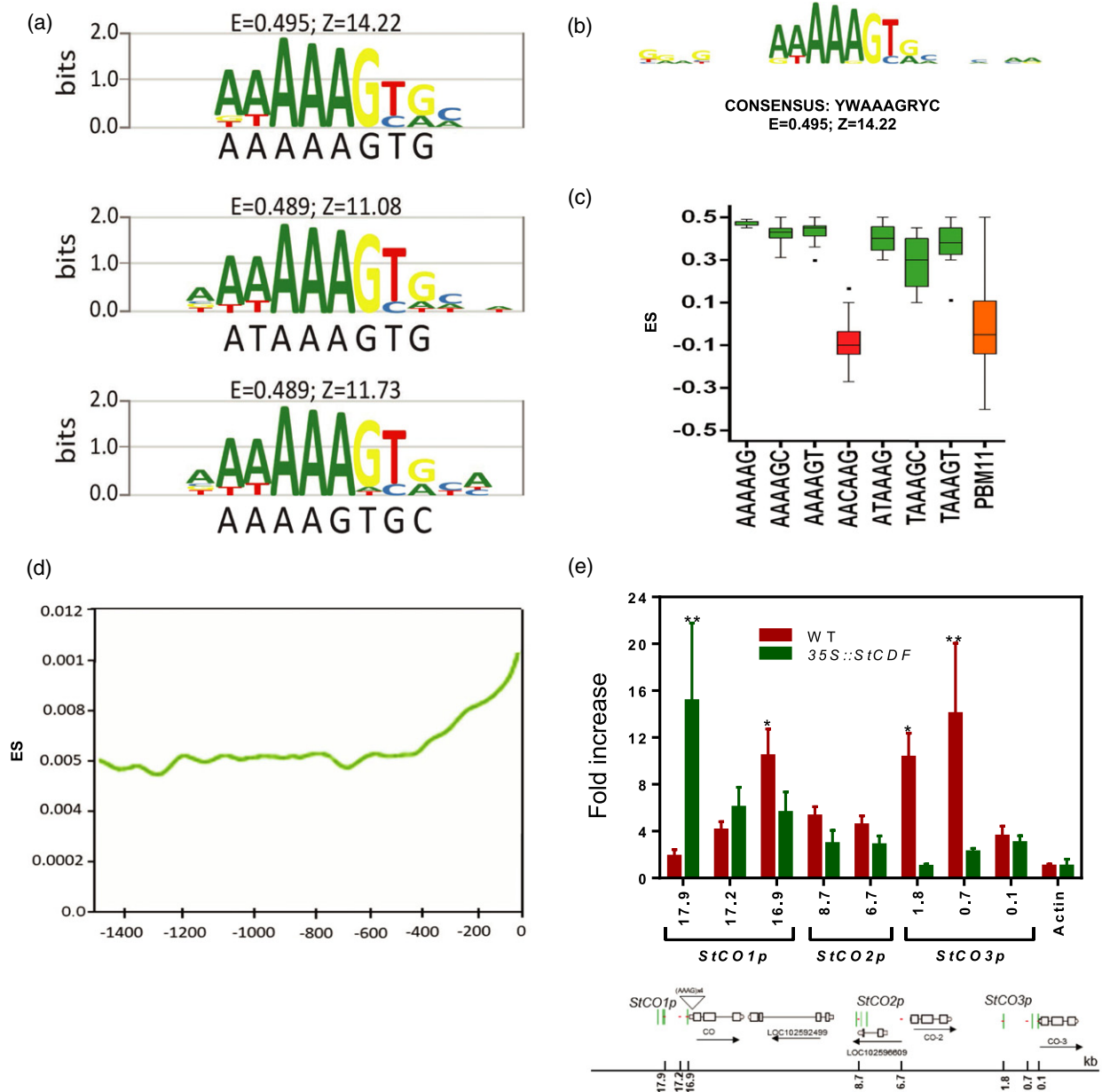


Figure 1. StCDF1 binding specificity assessed by protein binding microarray (PBM) and chromatin immunoprecipitation (ChIP) quantitative polymerase chain reaction (qPCR).

(a) Three different secondary position weight matrices (PWM) representing motifs obtained in the experiment, with Z score indicated.
 (b) Representative conserved DNA binding site motif (YWAAAGRYC).
 (c) Box plot of enrichment scores (ES) of the elements indicated, determined by PBM; note the low enrichment score when the element is disrupted.
 (d) Plot showing the YWAAAGRYC motif average distribution and local enrichment probability using all possible promoters of annotated potato genes as the input. The x-axis represents the distance relative to the transcription start site (TSS). The y-axis represents the enrichment score (ES).
 (e) Binding interaction of StCDF1 in CO promoter through the AAAG binding motif evaluated by Chip-qPCR in WT *Solanum tuberosum* group *Andigenum* (WT) and 35S::StCDF1 plants. Values are averages of three biological replicates and regions with significant enrichment above the actin negative control are indicated (* $P < 0.05$, ** $P < 0.01$; Holm–Sidak multiple comparison test). The relative fold enrichment was calculated using the pre-immunized serum as a background control. A schematic description of the studied genomic region is presented below. Red dots and numbers represent the qPCR primer pairs and green vertical bars represent putative StCDF1 binding sites in the *StCO1*, *StCO2* and *StCO3* promoters. All samples were collected at ZT3 under short days.

delays flowering in *Arabidopsis* (Kloosterman *et al.*, 2013). From these experiments it may be expected that silencing *StCDF1* gene expression would produce a phenotype with

delayed tuberization, but only if this transcription factor acts non-redundantly on the specific downstream tuberization signal transduction pathway. To check our hypothesis,

we made an *StCDF1*-specific RNAi construct and transformed it into the diploid potato clone carrying the homozygous wild-type *StCDF1.1* allele (CE3027). Ten transgenic potato plants were grown in the glasshouse and periodically checked for tuberization together with untransformed controls in three replicates. The CE3027 control began to tuberize 14 weeks after planting, under long-day conditions. All plants were grown until 18 weeks after planting. Six of the 10 transgenic lines did not produce any tubers (or swelling stolons). The remaining four transgenic plants had between one and three tubers and a mean total tuber fresh weight of 9.4 g per plant, compared with an average of six tubers and a mean total tuber fresh weight of 42.9 g per plant in the control plants (Table S1). The *StCDF1* RNAi plants were otherwise phenotypically normal in their growth habit and flowered at the same time as the non-transformed controls. We analysed the expression of the *StCDF* genes that are phylogenetically closest to *StCDF1*: *StCDF2* and *StCDF3* (Figure S2). Interestingly, although *StCDF1* expression was significantly downregulated in the *StCDF1* RNAi lines, the expression of both *StCDF2* and *StCDF3* were upregulated, compared with the controls (Figure 2a). We therefore checked the expression of these two homologues in the *35S:StCDF1.2* overexpression lines and found that *StCDF2* was downregulated in a light-stable version whereas *StCDF3* was markedly downregulated (Figure 2). Overall, these results showed first that *StCDF1* non-redundantly promotes tuberization and second that *StCDF1* appears to be a master regulator of a potato gene network also comprising other *StCDF* genes.

The *StCDF1* locus also codes for an antisense lncRNA called *StFLORE*

Recently, a *CDF5* lncRNA was identified in Arabidopsis, and molecular analysis showed that *FLORE* and *AtCDF5* exhibit antiphasic expression that reflects a mutual inhibitory regulation of controlling flowering time (Henriques *et al.*, 2017). Aiming to check whether the *StCDF1* locus would also encode an NAT-lncRNA, we analysed the RNA-Seq data from the DM1-3 516 R44 potato reference genome (PGSC 2011; Figure S2a). The reannotation of the strand-specific reads indicates an additional gene model in the *StCDF1* locus, possibly through the presence of an lncRNA on its antisense strand, similar to the *CDF5/FLORE* NAT pair in Arabidopsis. To confirm this, we performed strand-specific cDNA synthesis using four different primers to map the 3' end of the lncRNA transcript. PCR amplification in these four cDNA templates gave rise to only three products, allowing an approximate 3' end mapping of the transcript into the intron of the *StCDF1* gene (Figure S3b). When the transcription levels of *StFLORE* were tested over a 24-h time course under SDs in the diploid genotype CE3027 control, *StFLORE* peaked at night and showed an *StCDF1*-

antiphasic expression profile similar to *FLORE* expression in Arabidopsis (Figure S3c).

To visualize the spatial localization of both *StCDF1* and *StFLORE* transcripts, we fused an *StCDF1* or *StFLORE* upstream promoter region (2.0 and 3.3 kb, respectively) to the β -glucuronidase (*GUS*) gene for histochemical localization. After incubation and staining with X-Gluc, plants carrying *pStCDF1:GUS* showed clear macroscopic vascular staining (Figure 3a,b). Furthermore, stomatal guard cells staining was detected also in *pStCDF1:GUS* (Figure 3c). No staining was detected in vascular tissue and stomata guard cells in untransformed plants CE3027 (Figure S3d). The staining of *pStFLORE:GUS* partially overlapped with *pStCDF1:GUS*, as we detected vascular staining (Figure 3d, e). In comparison with *StCDF1* GUS staining, it was not possible to observe expression in stomata guard cells of *pStFLORE:GUS*. Thus, *StCDF1* and *StFLORE* cellular localization overlap in vascular tissue, where the main activity of *StCDF1* is controlling *StCO* genes and *StSP6A* gene expression, as expected (An *et al.*, 2004; Sharma *et al.*, 2016). Only *StCDF1* expression was found to be located in stomatal guard cells, however, indicating a specific regulatory role in this tissue.

StCDF1 locus is involved in drought stress responses

The *CDF* genes have been linked to abiotic stress responses to stresses such as drought, salt and extreme temperature (Corrales *et al.*, 2014; Fornara *et al.*, 2015; Corrales *et al.*, 2017). Using heterozygous potato plants carrying either *StCDF1.1/StCDF1.2* or *StCDF1.1/StCDF1.3*, compared with the homozygous *StCDF1.1/StCDF1.1* (CE3027) allelic configuration, we tested whether these potato clones show differences in tolerance to drought stress. The results show that the clones carrying a single copy of the *StCDF1.3* allele were significantly less tolerant to water-limiting conditions compared with either the heterozygous *StCDF1.1/1.2* or the homozygous *StCDF1.1* controls (Figure 3f,g). To further understand the impact of the different *StCDF1* allele combinations, we generated diploid potato genotypes that were *StCDF1.3* homozygotes and *StCDF1.2/StCDF1.3* heterozygotes. These plants were obtained from a cross between the diploid clones E and RH (see Experimental procedures). The presence of the homozygous *StCDF1.3* allele results in very early tuberization and leads to extremely weak plants with a stunted growth habit, compared with the parental controls (Figure S3e). We also analysed plants with an *StCDF1.2/1.3* allele combination and these plants had fewer branches and a smaller size than the control CE3027 (Figure S3e). *StCDF1.2* carries a 7-bp insertion, whereas *StCDF1.3* carries a transposon insertion of 860 bp; however, both insertions are situated in the C-terminal region of *StCDF1* and both result in a very similar functional truncated protein (Kloosterman *et al.*, 2013) (Figure 3h). We hypothesized that the

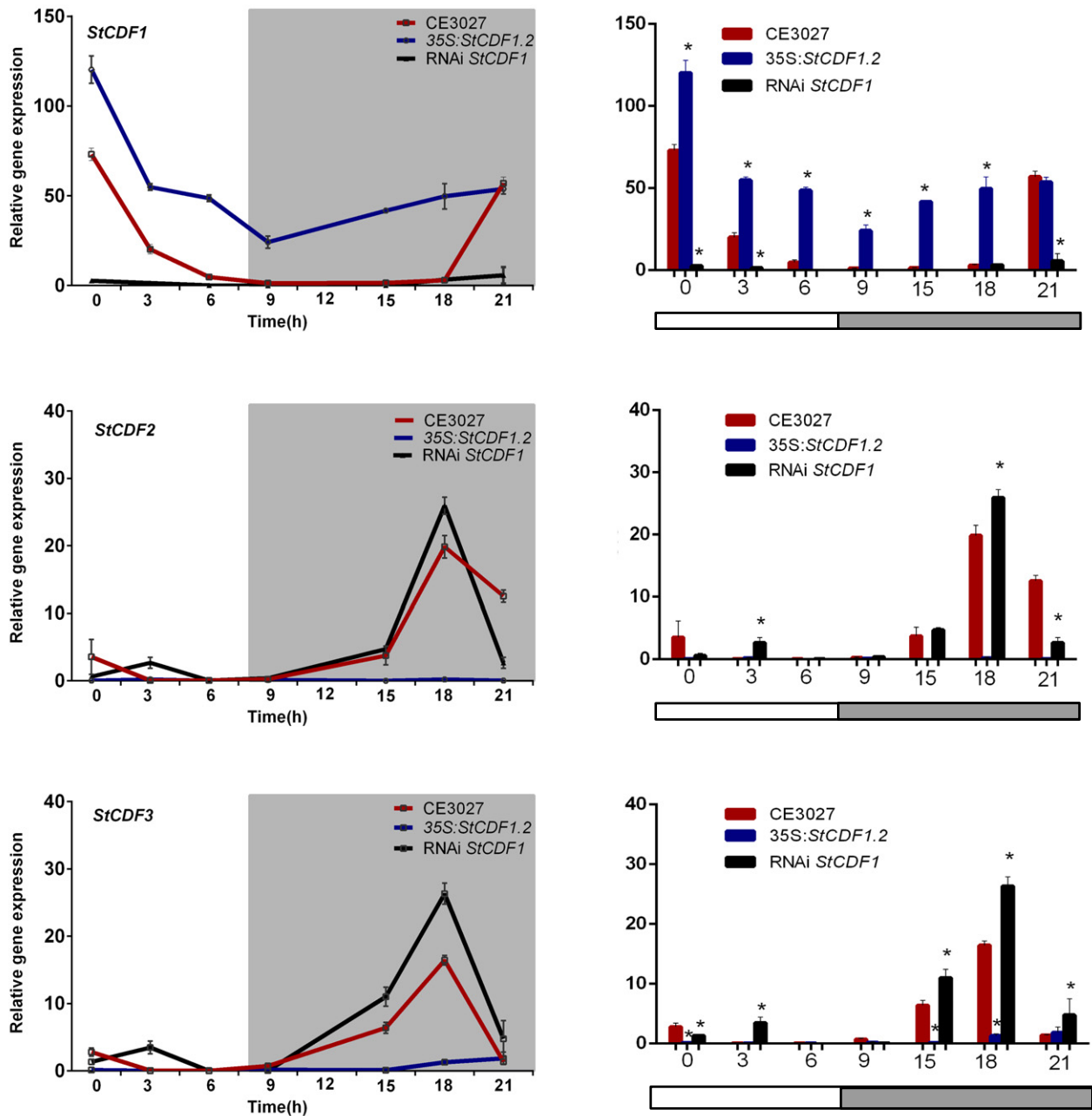


Figure 2. *StCDF1* knock-down non-redundantly delays tuberisation. Relative gene expression profile of *StCDF1* and its close CYCLING DOF FACTOR family members *StCDF2* and *StCDF3* in two *StCDF1* RNAi lines and two *35S:CDF1.2* lines during a 24-h time course under short-day conditions. CE3027 was used as a control for 1.1/1.1 allele combination. Error bars: means \pm SEMs, with $n = 3$ biological replicates. Significant changes of gene expression compared with control CE3027 (1.1/1.1): * $P \leq 0.05$.

different insertions have a differential effect on *StFLORE* transcription, which we tested by reverse-transcriptase qPCR (qRT-PCR) using strand-specific cDNA templates of the various allelic variants from *StCDF1* at zeitgeber time 9 (ZT9; peak of *StFLORE* expression) under SD conditions. *StFLORE* expression could not be detected in the *StCDF1.3*

homozygotes (Figure 3i), probably as a result of the 860-bp displacement of the *StFLORE* promoter (Figure 3g). Furthermore, heterozygotes carrying one copy of the *StCDF1.3* allele showed lower *StFLORE* expression than the control, whereas *StCDF1.1/1.2* heterozygotes showed an even higher *StFLORE* expression than the control (Figure 3i).

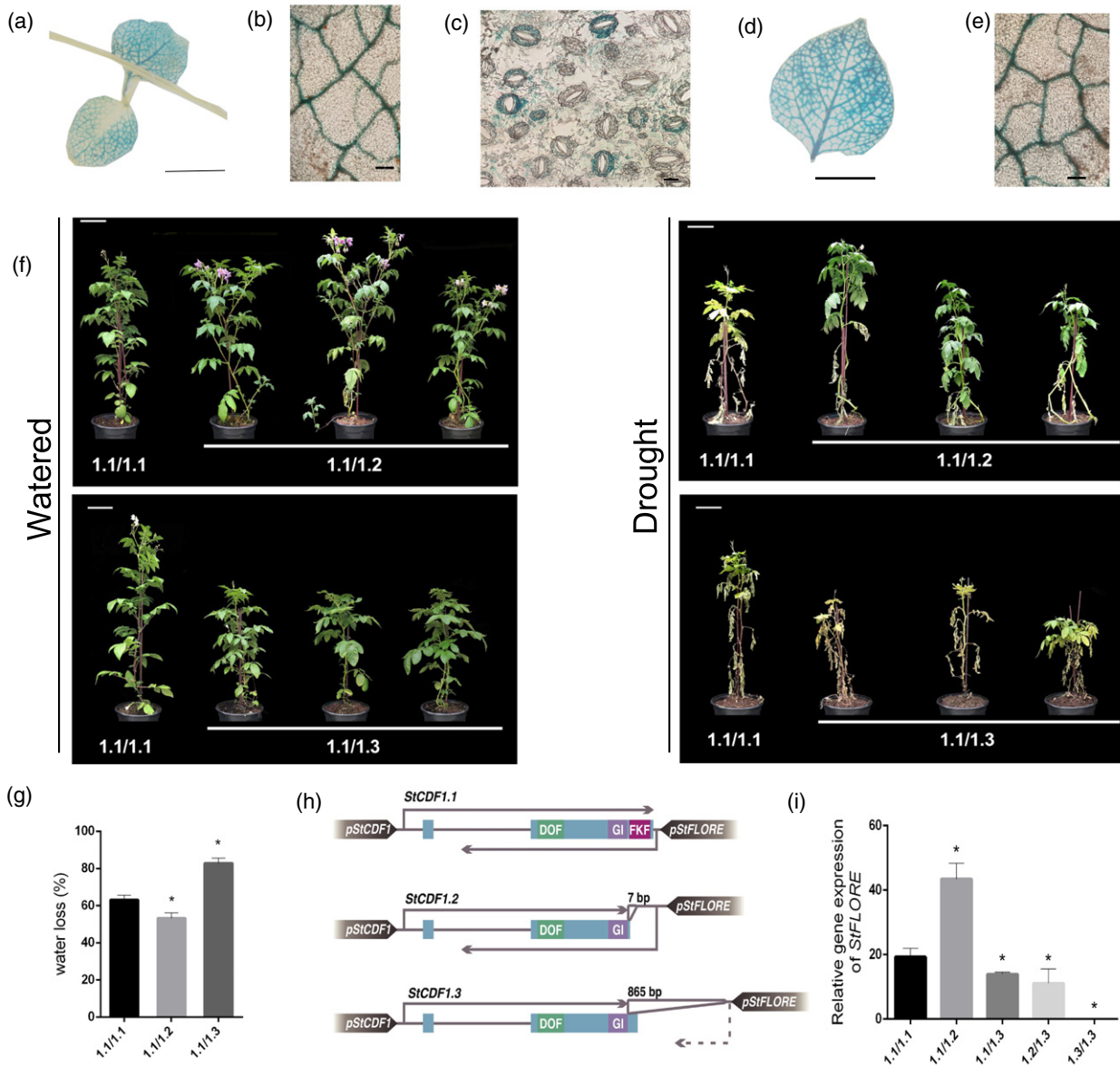


Figure 3. *StCDF1* locus encodes for an antisense lncRNA called *StFLORE*.

(a–e) β -Glucuronidase (GUS) staining of *pStCDF1:GUS* (#12 and #7) and *pStFLORE:GUS* (#12 and #15) plants, showing *StCDF1* localization in young leaf (a–b) and stomata guard cells (c), and *StFLORE* localization in young leaf (d–e). *StCDF1* and *StFLORE* were both expressed in vascular tissue. Scale bars: (a) 0.5 cm; (b) 20 \times , 20 μ m; (c) 40 \times , 20 μ m; (d) 0.5 cm; (e) 40 \times , 20 μ m.

(f) Plants with different allele combinations of *StCDF1* under normal (left) and drought conditions (right). We show 1.1/1.2 (top) and 1.1/1.3 (below) allelic combinations for *StCDF1*. CE3027 was used as a control for 1.1/1.1 allele combination. $n = 3$ biological replicates. * $P < 0.05$, with respect to control.

(g) Water loss after drought-stress conditions. CE3027 was used as control for 1.1/1.1 allele combination. $n = 14$ biological replicates. * $P < 0.05$, with respect to control. For further details, see Experimental procedures.

(h) Schematic representation of the three *StCDF1* alleles. The protein coding region is shown as blue boxes and the relevant domains are shaded in green (DOF domain), lilac (GI binding region) and purple (FKF binding region). Transcripts of *StCDF1* and *StFLORE* are shown as grey arrows. The non-functional *StFLORE* transcript in the allelic variant *StCDF1.3* is represented as a dotted line. Insertions are indicated as grey triangles (7 bp in *StCDF1.2* and 865 bp in *StCDF1.3*). Putative promoters of *StCDF1* and *StFLORE* are shown as grey arrowheads. *StFLORE* starts at 2400 bp and ends around 1320 bp from *StCDF1* TSS. *pStFLORE* is located downstream from the stop codon of *StCDF1*.

(i) Real-time analysis of *StFLORE* expression for different *StCDF1* allele compositions at ZT9 under short days; 1.3/1.3 allele composition did not show *StFLORE* expression. Error bars: means \pm SEMs, with $n = 3$ biological replicates. * $P < 0.05$, with respect to control.

These results indicate that the presence of the *StCDF1.3* allele disrupts *StFLORE* expression and results in detrimental growth and reduced fitness in potato.

To ascertain the abiotic stress susceptibility of the potato *StCDF1* locus, we exposed *StCDF1* RNAi plants to drought stress. The *StCDF1* RNAi showed a dramatic increase in drought tolerance (Figure 4a). *StCDF1* RNAi had a lower water loss rate under drought stress and a lower number of tubers under both optimal water conditions and drought treatment, compared with the control (Figure 4b,c). In parallel, we grew plants overexpressing *StCDF1.2*, which showed a weaker phenotype even under optimal water conditions (Figure S4a). Sequence analysis of the putative *StFLORE* promoter reveals the presence of multiple *StCDF1* binding motifs (Figure S5). We therefore also checked *StFLORE* expression in the *StCDF1.2* overexpression plants as well as the *StCDF1* RNAi plants in a 24-h time course under SD conditions. We found that the highest peak of *StFLORE* at ZT9 was twofold upregulated in *StCDF1* RNAi plants compared with the controls (Figure 4d), consistent with the high level of drought tolerance of these plants (Figure 4a). In contrast, plants overexpressing *StCDF1* showed a 30-fold decrease of *StFLORE* expression at both ZT6 and ZT12, compared with the control (Figure 4d).

Taken together, the expression analysis indicates a repression of *StFLORE* expression by *StCDF1*. To check whether this regulation is direct, we performed a ChIP-qPCR assay using CE3027 plants expressing a GFP-tagged *StCDF1* under the phloem-specific promoter *SUC2*. After the ChIP assay, an enrichment of chromatin was visible in the proximal region (P1) of the transcription start site of *StFLORE* (Figures 4e and S5b). Enrichment values are close to those of the *StCDF3* promoter, used as a positive control, and probably under similar transcriptional regulation by *StCDF1*. From these results, we can conclude that *StCDF1* negatively regulates *StFLORE* by directly binding to its promoter.

Increasing *StFLORE* expression confers drought tolerance

To gain more insight into *StFLORE* function we overexpressed and knocked down *StFLORE* gene expression. We constructed an *StFLORE* transcript, driven by the cauliflower mosaic virus (CaMV) 35S promoter (*35S:StFLORE*) and a CRISPR-Cas9 cassette targeting 1 kb of the *StFLORE* promoter using four RNA guides, including putative DOF-binding motifs, proximal to the lncRNA start of transcription (Figure S5a). We found that using guides 1, 2 and 3, produced deletions of 770 and 952 bp, named $\Delta pStFLORE\#22$ and $\Delta pStFLORE\#53$ (Figure S5b). Under normal growing conditions, $\Delta pStFLORE$ plants showed a delay in development, with smaller leaves and lower heights compared with the controls, whereas overexpressing *StFLORE* did not show any difference compared with the controls (Figure S6a). Regarding tuberization,

$\Delta pStFLORE$ plant lines showed early tuberization and a slightly higher number of tubers compared with the control (Figure S6b). *35S:StFLORE* showed a decrease in tuber number and also a delay in tuberization compared with the control (Figure S6b). *35S:StFLORE* and $\Delta pStFLORE$ plants were exposed to 2 weeks of moderate drought stress (see Experimental procedures). *35S:StFLORE* plants were more drought tolerant and $\Delta pStFLORE$ plants were more susceptible to drought stress, compared with control CE3027 plants (Figure 5a,b). In *35S:StFLORE* overexpression plants, water loss was lower compared with that of control CE3027 plants and they had the lowest number of tubers under drought stress, whereas $\Delta pStFLORE$ plants had a slightly higher water loss under drought stress compared with controls and showed no differences in tuber numbers compared with controls under drought conditions (Figures 6b and S6c).

Finally, we analysed the relative expression of *StFLORE* and *StCDF1* transcripts in our transgenic plants during a 24-hour time course under SD conditions. We found that the *35S:StFLORE* plants had a similarly high expression level of *StFLORE* as the *StCDF1* RNAi plants, peaking at ZT9, under SDs (Figures 4d and 5c). *StCDF1* expression was lower in the *35S:StFLORE* plants compared with the controls (Figure 5d). In contrast, $\Delta pStFLORE$ plants showed on average a sixfold lower expression of *StFLORE* at ZT6 and a threefold lower expression at ZT9 and ZT12, compared with controls (Figure 5c), and a higher expression of *StCDF1* at ZT0 (1.4-fold), ZT6 (13-fold), ZT9 (8-fold), and ZT12 and ZT15 (22-fold), compared with controls (Figure 5d).

In *35S:StFLORE* plants, we also checked for the expression of *StCDF2* and *StCDF3* in a 24-h time course under SD conditions. We found that these two other *StCDF* family members showed slightly higher expression than the controls, which is likely linked to the lower expression of *StCDF1*. In $\Delta pStFLORE$ plants there was a reversed pattern, where the expression of *StCDF2* and *StCDF3* was slightly lower than that observed in controls (Figure S7a,b). In summary, we suggest that *StCDF1* and *StFLORE* are subject to regulatory feedback: *StCDF1* is likely to regulate *StFLORE* expression through the binding of DOF motifs in its promoter, whereas *StFLORE* acts as a NAT on the *StCDF1* transcript. Furthermore, increasing *StFLORE* expression in *35S:StFLORE* transgenics confers drought tolerance to these plants. Finally, the inverse expression pattern of *StCDF2* and *StCDF3*, compared with *StCDF1*, indicates that *StFLORE* primarily regulates *StCDF1* rather than the other two family members.

Drought response is conferred by the regulation of stomatal guard cell dynamics, impacting plant water loss

We have shown that *StCDF1* RNAi and *35S:StFLORE* enhanced resilience to drought. Aiming to establish the

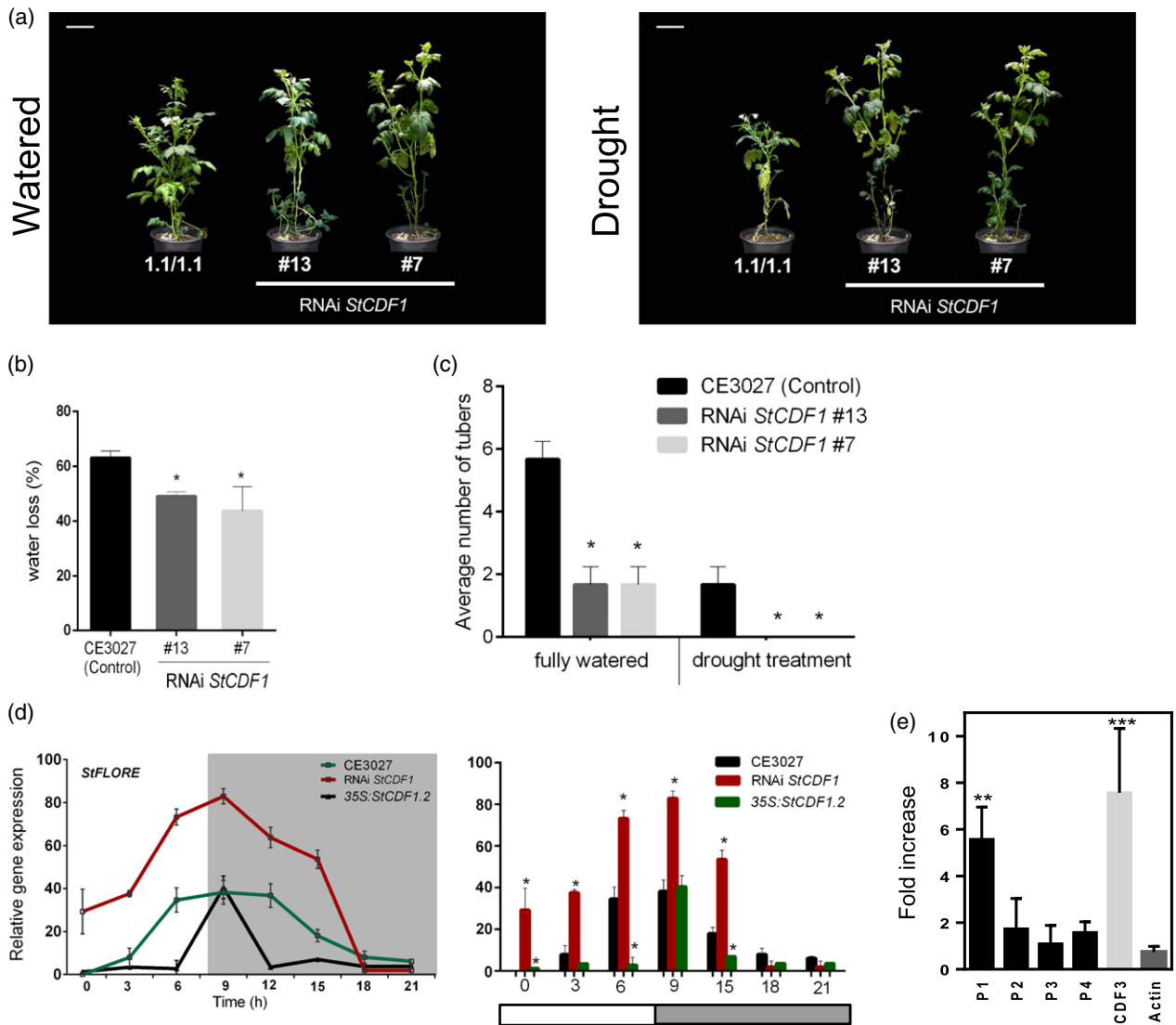


Figure 4. *StCDF1* knock down shows enhanced drought tolerance and increased *StFLORE* expression.

(a) CE3027 (1.1/1.1) untransformed control and two representative *StCDF1* RNAi transgenic lines under fully watered conditions (left) and after 10 days of drought (right).

(b) Water loss percentage after drought-stress conditions in *StCDF1* RNAi lines. CE3027 (1.1/1.1) untransformed was used as a control. Error bars: means ± SEMs, with *n* = 3 biological replicates. **P* < 0.05, with respect to control. For further details, see Experimental procedures.

(c) Average number of tubers under drought and fully watered conditions in *StCDF1* RNAi lines. CE3027 (1.1/1.1) untransformed was used as a control. Error bars: means ± SEMs, with *n* = 3 biological replicates. **P* < 0.05, with respect to control.

(d) Relative gene expression of *StFLORE* using two representative lines of *StCDF1* RNAi and *35S:StCDF1.2* during a 24-h time course under optimal water conditions in short days. Untransformed CE3027 (1.1/1.1) was used as a control. Error bars: means ± SEMs, with *n* = 3 biological replicates. Significant changes of gene expression compared with control CE3027 (1.1/1.1): **P* ≤ 0.05.

(e) *StCDF1* physically associates with *StFLORE* promoter detected by ChIP-qPCR in *SUC2:GFP-CDF1* plants. Values are averages of three biological replicates + SDs. Regions with significant enrichment above actin negative control are indicated (***P* < 0.01; ****P* < 0.001, adjusted *P* value, Dunnett's multiple comparison test). The relative fold enrichment was calculated using GFP alone with transformed plants as a control. As a positive control a region with a theoretically high number of *StCDF1* binding sites in the *StCDF3* promoter was used. All samples were collected at ZT4 under long days. Amplicons are representative of consecutive genomic regions in the promoter, from proximal (P1) to distal (P4) *StFLORE* transcription start site.

physiological basis of this drought tolerance, we measured stomatal behaviour. We tested the stomatal aperture under ABA treatment in our transgenic plants. Our results show that although *StCDF1* RNAi and *35S:StFLORE*

overexpression plants respond to ABA with lower stomata aperture values, *35S:StCDF1.2* and $\Delta pStFLORE$ lines were insensitive to ABA treatment (Figure 6a,b). In addition, our results revealed that *StCDF1* and *StFLORE* also affect

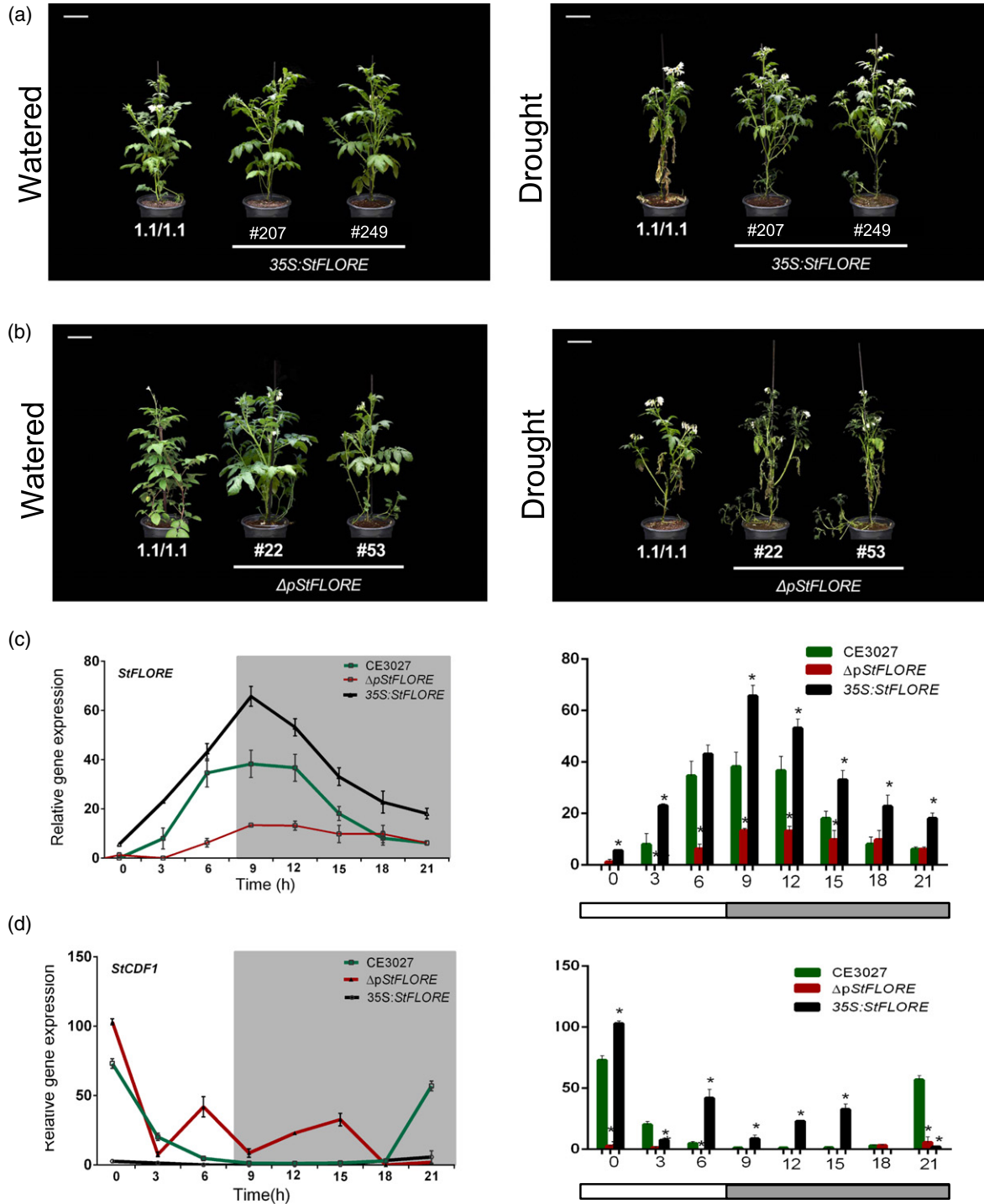


Figure 5. Analysis of CRISPR/Cas9 p*StFLORE* plants and overexpressing *StFLORE* lines.

(a) CE3027 (1.1/1.1) untransformed control (left) and two representative 35S:*StFLORE* lines after 10 days of drought (right). Error bars: means ± SEMs, with $n = 3$ biological replicates.

(b) CE3027 (1.1/1.1) untransformed control (left) and two representative Δ*pStFLORE* transgenic lines after 10 days of drought (right). Error bars: means ± SEMs, with $n = 3$ biological replicates.

(c) Relative gene expression of Δ*pStFLORE* and 35S:*StFLORE* during a 24-h time course under optimal water conditions in short days. The untransformed CE3027 (1.1/1.1) from Figure 4(b) was used as a control. Error bars: means ± SEMs, with $n = 3$ biological replicates. Significant changes of gene expression compared with control CE3027 (1.1/1.1): * $P \leq 0.05$.

(d) Expression of *StCDF1* in Δ*pStFLORE* and 35S:*StFLORE* during a 24-h time course under optimal water conditions in short days. Error bars: means ± SEMs, with $n = 3$ biological replicates. CE3027 (1.1/1.1) untransformed from Figure 2(a) was used as a control. Significant changes of gene expression compared with control CE3027 (1.1/1.1): * $P \leq 0.05$.

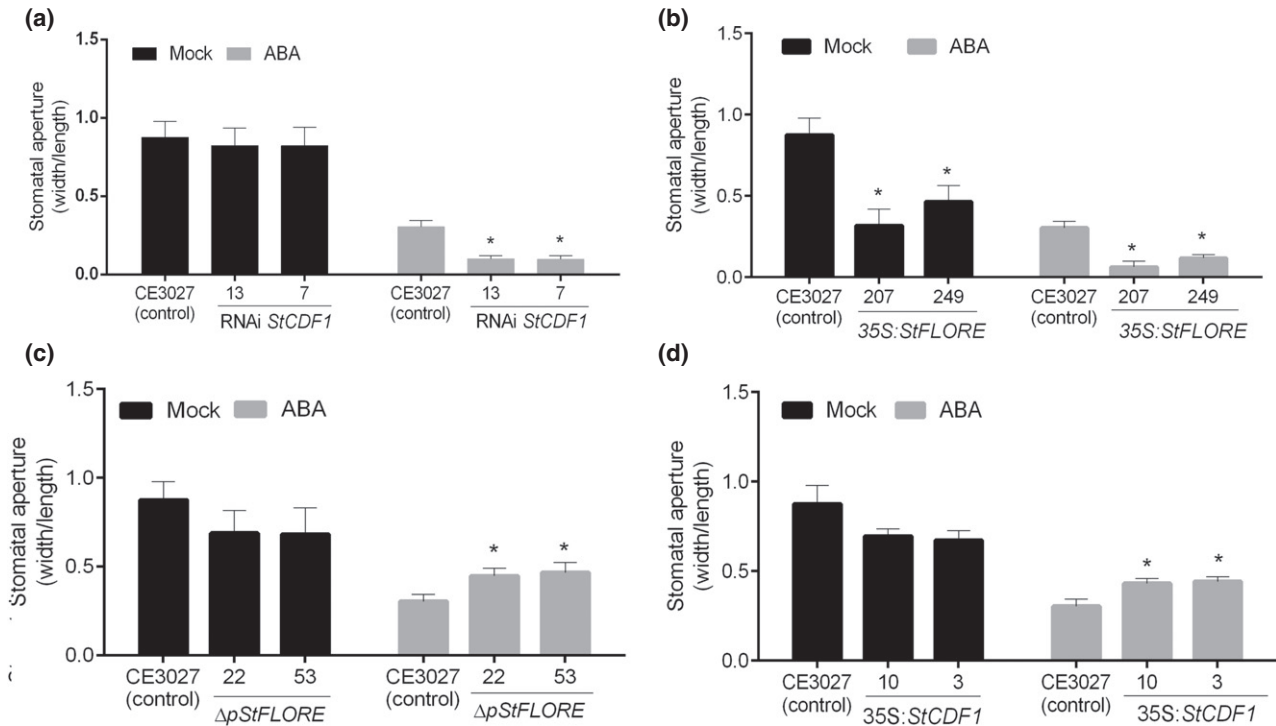


Figure 6. Stomata opening is affected in plants with higher or lower *StCDF1* and *StFLORE* expression.

(a) Stomatal pore aperture of *StCDF1* RNAi and *35S:StCDF1.2* under ABA treatment, compared with untransformed CE3027 (1.1/1.1) as a control. Error bars: means \pm SEMs, with $n = 3$ biological replicates. * $P < 0.05$, with respect to control. For further details, see Experimental procedures.

(b) Stomatal aperture ratio of CRISPR/Cas9 *StFLORE* promoter ($\Delta pStFLORE$) and *35S:StFLORE* under ABA treatment, with untransformed CE3027 (1.1/1.1) as a control. Error bars: means \pm SEMs, with $n = 3$ biological replicates. * $P < 0.05$, with respect to control. For further details, see Experimental procedures.

stomata density and size (Figures S8 and S9; Table S2). For instance, *StCDF1* RNAi and *35S:StFLORE* overexpression plants have higher stomatal density but smaller guard cell size, and *35S:StCDF1* overexpression plants have lower stomatal density but larger stomatal guard cells (Table S2). Moreover, previously we found that *StCDF1* RNAi and *35S:StFLORE* overexpression plants also have the lowest values of water loss under drought stress (Figures 4b and S6c). Taken together, these results show that our tolerant transgenic *StCDF1* RNAi and *35S:StFLORE* overexpression plants are able to decrease their water loss not only by responding to ABA but also through the regulation of stomata size and number.

DISCUSSION

Cycling DOF transcription factors are transcriptional repressors that, together with TOPLESS, regulate downstream initiators of reproductive development (Imaizumi *et al.*, 2005; Abelenda *et al.*, 2014; Wu *et al.*, 2017). In potato, this includes the indirect activation of tuber development (Kloosterman *et al.*, 2013). We show here that *StCDF1* protein binds to canonical DOF motifs in the promoter regions of a tandem array of three potato *CONSTANS* genes located on chromosome 2. The repression of these *StCO* genes, and especially of *StCO1*, by *StCDF1*

is likely to prevent the induction of an *FT*-like repressor (*StSP5G*) of the tuberigen *StSP6A*, making *StCDF1* an indirect positive regulator of tuberization. This is similar to the situation in *Arabidopsis* where *CDF1* also represses *CO* (Song *et al.*, 2012). Unlike *Arabidopsis*, however, where a quadruple *CDF* mutant is required to exhibit early flowering and be photoperiod insensitive (Fornara *et al.*, 2009), we show here that *StCDF1* is able to affect tuberization by itself. This confirms that a single potato *CDF* homologue has evolved specifically to regulate tuberization.

In addition to its regulation of potato *StCO* and *StSP5G* gene expression, *StCDF1* represses the expression of *StCDF2* and *StCDF3*. We noted from an analysis of PGSC RNA-Seq data that the *StCDF4* locus also has a secondary gene model that is very similar to that of *StCDF1*, indicating the possible presence of an lncRNA transcript for this locus (PGSC, 2011). Recently, Kondhare *et al.* (2019) showed that *StCDF1* gene expression is regulated by a BEL1-like protein (*StBEL5*). Interestingly, we found that the KNOX-partner of *StBEL5* (*StPOTH1*) is downregulated in *35S:StCDF1* plants, indicating complex upstream regulatory circuitry that will require further analysis.

As shown for *Arabidopsis* (Henriques *et al.*, 2017), potato *StCDF1* also has an lncRNA natural antisense transcript, *StFLORE*. In potato, the antiphasic expression pattern of

these transcripts and the binding interaction of StCDF1 in the *StFLORE* promoter indicates that *StCDF1* modulates the expression of the *StFLORE* transcript. In homozygous *StCDF1.3* plants, we do not detect any *StFLORE* transcript. The transposon insertion in this natural allele, displaces the promoter thereby disrupting the functional *StFLORE* lncRNA transcript, in addition to truncating the StCDF1 protein. Both natural allelic variation and engineered *StFLORE* promoter knockdowns (*StCDF1.3* homozygotes and CRISPR-cas9 deletions of the *StFLORE* promoter, respectively) have a profound effect on plant fitness. Conversely, the elevation of *StFLORE* expression, either by a reduction of *StCDF1* expression or by the overexpression of the *StFLORE* transcript itself, leads to an enhanced tolerance to abiotic stress. Multiple links have been found between abiotic stress tolerance and *CDF* gene expression, including drought, salt and temperature stresses (Corrales *et al.*, 2014; Fornara *et al.*, 2015; Corrales *et al.*, 2017; Renau-Morata *et al.*, 2017). Our data from both genetic studies of allelic variants of *StCDF1* and the transgenic plants with differences in gene expression of *StCDF1* or *StFLORE* indicate that both components are likely to be responsible for the drought-tolerance phenotype in potato. The drought-tolerance phenotype of *StCDF1* RNAi and *35S:StFLORE* could be a consequence of the late maturity of the plants (Spitters and Schapendonk, 1990; Aliche *et al.*, 2019). Interestingly, a preponderance of DOF binding motifs has been detected in promoters of stomatal guard cell-expressed genes (Plesch *et al.*, 2001); however, a direct mechanistic link of *StCDF1* and *StFLORE* with the regulation of stomatal guard cell opening and closing remains unclear on a molecular level. Our results from stomatal density and stomatal guard cell sizes in our tolerant transgenics, *35S:StFLORE* and *StCDF1* RNAi plants, concur with previous studies where water deficit leads to a decrease in stomatal size (Cutler *et al.*, 1977; Quarrie and Jones, 1977; Spence, 1987) and an increase in stomatal density (McCree and Davis, 1974; Cutler *et al.*, 1977; Yang and Wang, 2001; Zhang *et al.*, 2006), with stomatal density linked to water-use efficiency (Yang *et al.*, 2007). The co-expression of *StCDF1* and *StFLORE* in the vasculature indicates a primary role for *StFLORE* regulation of *StCDF1* in this tissue. If not a result of technical limitations in the *promoter:GUS* approach, the lack of *StFLORE* expression in stomatal guard cells indicates that there may be further intermediates affecting the influence of this transcript, however. Significant differences in the expression of ABA biosynthesis genes in *StFLORE* overexpression and knockout plants, as well as the transcriptional responsiveness of *StFLORE* gene expression to ABA, may provide an interesting lead for this signalling pathway. Nevertheless, we present data from natural *StFLORE* promoter knockdowns, CRISPR-Cas-9 mutants and overexpression transgenics indicating that *StFLORE* regulates stomatal guard cell dynamics. There is

a vast volume of literature that links lncRNAs to abiotic stress, however, only a few of them have been fully characterized (Matsui and Seki, 2019). Our results show that the expression of the *StFLORE* lncRNA is regulated by promoter binding by StCDF1 protein, and in turn this influences stomatal aperture and guard cell size. These effects are not linked to the earliness effect of *StCDF1* truncation alone, as the *StCDF1.2* variant appears not to have adverse effects on *StFLORE* expression or plant fitness under normal or drought-stress conditions.

Earliness of tuberization and life-cycle length are critical traits for plant breeding and agriculture, as they have profound effects on yield and production in various geographic locations. This importance is accentuated in the new true hybrid breeding programmes where life-cycle length is essential when planning to start with true-seed potato material. Potato crosses based solely on the phenotype do not guarantee avoiding early allelic variants of *StCDF1* in the progeny. Moreover, knowing that a single *StCDF1.3* allele produces a negative effect on fitness under abiotic stress situations, it is indispensable to develop specific molecular markers to distinguish the early alleles in breeding programmes so as to not introduce adverse effects of knocking down the *StFLORE* transcript.

EXPERIMENTAL PROCEDURES

Potato material and growth conditions

Potato plants with different allelic combinations of *StCDF1* were obtained from C × E diploid clones. Clone C (USW5337.3) is a hybrid between *Solanum phureja* PI225696.1 and *S. tuberosum* dihaploid USW42. Clone E (VPH4 77.2102.37) is the result of a backcross between clone C and *Solanum vernei-S. tuberosum* clone VH3 4211. RH (RH89-039-16), a diploid heterozygous potato clone, and E were crossed to obtain the 1.3/1.3 allelic combination of *StCDF1*. The C × E (CE3027, CE605 and CE630) and RH × E (RHE25) progeny, together with transgenic plants generated in this study, were vegetatively propagated and grown *in vitro* on MS medium supplemented with 2% w/v sucrose (Murashige and Skoog, 1962). Two-week-old plants were planted in soil and grown either in the glasshouse at 23°C under long days (LDs) or in controlled-environment chambers at 2°C under SDs (with 8 h of light and 16 h of dark). The plants used for this study are listed in Table S3, including CE3027, CE605, CE630 and RHE25, which possess 1.1/1.1, 1.1/1.2, 1.1/1.3 and 1.3/1.3 allelic compositions, respectively, which were used for molecular analysis.

Drought exposure

After 2 months of growing in the glasshouse, the C × E population and transgenic plants were divided into two treatments: optimal irrigation and drought stress. Optimal irrigation was considered to be, manual watering every 2 days, corresponding to 100% field capacity. Plants grown under drought conditions were also irrigated every 2 days, but with decreasing field capacities of 60% for 5 days and 40% for the following 5 days. In total, these plants were exposed to 10 days of drought stress. After approximately 120 days after sowing, tuber number and tuber fresh weight were measured for all

individuals grown under optimal irrigation and drought treatments. To obtain tuberization timing we check the tubers from week 10, when they begin to tuberize, onwards. To measure water loss under drought conditions, fully developed leaves of control CE3027 and transgenic plants were cut after 10 days of drought treatment and exposed at room temperature. The leaves were weighed 4 h after being cut. Water loss (%) was calculated as [(fresh weight – dry weight after 4 h)/fresh weight] × 100 of eight leaves under drought stress (Campo *et al.*, 2012). To measure water loss under drought conditions, fully developed leaves of control CE3027 and transgenic plants were cut after 10 days of drought treatment and exposed at room temperature. The leaves were weighed 4 h after being cut. Water loss (%) was calculated as = (fresh weight-dry weight after 4 h)/fresh weight × 100) of 8 leaves under drought stress.

Physiological evaluation

Stomatal aperture was measured as reported previously (Roelfsema and Prins, 1995; Desikan *et al.*, 2005). Briefly, the leaves of 4-week-old plants growing in a glasshouse were cut and first submerged into MOCK solution (a buffer that favours stomata opening). After 3 h, half of the leaves were submerged in ABA (10 μM) and the other half was kept in the MOCK solution as a control (Eisele *et al.*, 2016). Stomatal aperture in leaves treated with ABA and Mock solution was calculated by measuring width over length from the stomata aperture. The reading was performed for a total of 30 stomata in four leaves per genotype under the microscope, with a 40× magnification. Furthermore, we calculated stomata density as stomata number per mm² area and stomata size by using the oval area formula (μm²).

Histological analysis

For the *pStFLORE:GUS* construct, a 3.3-kb fragment upstream of the 5' transcription start site of *StFLORE* (for further details of the exact position, see Table S4) was amplified by using 5'-CACCT-CATAAGTGGAGTAAGCCTTACGA-3' and 5'-TCACTAAT-TATGTTGCTCATCCT-3' and cloned into pENTR TOPO vector to generate the ENTRY Gateway® clones first, and then transferred to pKGFWS7 following the manufacturer's instructions. For the promoter *StCDF1:GUS* construct, a 2-kb upstream *StCDF1* was amplified by PCR using 5'-CACCCAATATGAACTTTGTTGTATA-TAAAAATATAAA-3' and 5'-GATGAAGAAGAAAAAGGGTTTTAGA-3' and then cloned following the same procedures as described above. Both the *pStFLORE:GUS* and *pStCDF1:GUS* constructs were introduced into *Agrobacterium tumefaciens* strain GV3101 and transformed into diploid potato CE3027 and *Solanum tuberosum*, respectively. The subcellular localization of transgenic lines were used for GUS staining, as described previously (Jefferson *et al.*, 1987). As a negative control, untransformed CE3027 was stained with GUS. Photos were taken of 3-week-old transgenic plants under the microscope with a magnification of 40× and 20× for stomata and vasculature cells visualization, respectively.

Generation of constructs and transformation

RNAi lines (*StCDF1#7* RNAi and *StCDF1#13* RNAi) were constructed by cloning the *StCDF1* cDNA fragment using 5'-CACC ATGCTGAAGTTAGAGATCCTGCT-3' and 5'-GACACAAGAACC GCTATGC-3' that contained the full coding sequence (Table S4). The inverted repeat is assembled in the binary vector by a two-step cloning process with specific restriction enzyme sites (Karimi

et al., 2002). The fragment was subsequently recombined into the binary vector pK7GWIWG2 using LR clonase (Invitrogen, now ThermoFisher Scientific, <https://www.thermofisher.com>) and transformed into TOP10 *E. coli* cells. The presence of the insert was confirmed by PCR amplification and the direction was verified by digestion and sequencing. Successful constructs were then transformed by electroporation into *Agrobacterium tumefaciens* GV3101 and confirmed by PCR before genetic transformation.

A plasmid with the specific *SUC2* promoter was generated to obtain plants expressing GFP-CDF1.1 in the phloem. pALLIGATOR2pSUC2UTR_GW, kindly provided by G. Coupland, was used as a template to amplify the *SUC2* promoter with primers including *HindIII* and *XbaI* restriction sequences. The PCR product was cloned in pGEMTeasy, sequenced, digested with *HindIII* and *XbaI*, and ligated again in pGWB406 after digestion and excision of its 35S promoter with the same enzymes, obtaining the pGWB06SUC2 plasmid. Finally, LR recombination between *StCDF1.1* ORF in TOPO pENTR and pGWB06SUC2 was performed, and the final *SUC2:GFP-StCDF1.1* plasmid transferred to CE3027 plants. In parallel, an empty *SUC2:GFP-Stop* construct was created to transform plants and use them as negative controls.

The CRISPR/Cas9 knockout of the *StFLORE* promoter was performed by using Golden Gate cloning. We selected four sgRNAs along 1.5 kb of the *StFLORE* promoter including *StCDF1* binding sites (see Figure S5). The four sgRNA scaffold clones with 20-bp target sequences were previously obtained by PCR using a pair of synthetic specific primers using gRNA_GFP_T1 as a template. They were recombined with *pICH47732:NOSp:NPTII-OCST*, *pICH47742:35Sp:Cas9-NOST*, the linker pICH41780 and cloned in pAGM4723 in a single-cut ligation reaction with *BbsI* and T4-ligase. (ThermoFisher Scientific). The final binary plasmid contained an *hCas9* gene under the CaMV 35S promoter and four single-guide RNAs (sgRNAs) under the control of the *AtU6* promoter.

To detect mutagenesis, we amplified by PCR using DreamTaq DNA polymerase (ThermoFisher Scientific), with fragments containing guides sg1, sg2, sg3 and sg4 with the forward primer 5'-TCCCTTTCTACTTCGATCTACCTC-3' and reverse primer 5'-CAGAGTCTTCAAGTTTTATAGTTGTGC-3' (Table S4). From 100 regenerated plants we obtained two transgenic plants (Δ p*StFLORE#22* and Δ p*StFLORE#53*) from which we amplified the 1.5-kb region upstream of the transcription site of *StFLORE* to clone into pGEMT Easy vector (Promega, <https://www.promega.com>), and 10 colonies from each transgenic plant were sent for sequencing with M13 primers. In all the plants tested, at least one colony carries the intact *StFLORE* promoter. From these transgenics, we checked that the *StCDF1* gene was not affected by our guides.

Overexpression plants of *StFLORE* (*35S:StFLORE#207* and *35S:StFLORE#249*) were constructed by amplifying the reverse complement from the *StCDF1* gene with the forward primer 5'-CACCGGAGAGTGTAGTAGGATT-3' and reverse primer 5'-CTACTCTTCAGATCCCATTG-3' (Table S4). The PCR-generated full-length sequence was cloned into pENTR TOPO vector and TOP10F cells were transformed according to the manufacturer's instructions (Invitrogen, now ThermoFisher Scientific). An LR recombination reaction was performed between the entry clone (pENTR TOPO) and the destination vector (pK7WG2), according to the manufacturer's protocols (Invitrogen, now ThermoFisher Scientific). Transgenic plants overexpressing *StCDF1.2* (*35S:StCDF1#3* and *35S:StCDF1#10*) were described previously (Kloosterman *et al.*, 2013).

RNA extraction and qRT-qPCR analysis

The samples were harvested and stored in liquid nitrogen until RNA extraction. The isolation of total RNA was performed with the RNeasy mini kit (Invitrogen, now ThermoFisher Scientific) following the corresponding protocol. DNA digestion was accomplished by DNase I (TaKaRa, <https://www.takarabio.com>), and the first-strand cDNA was obtained according to the manufacturer's instructions, by either superscript VI reverse transcriptase (Invitrogen, now ThermoFisher Scientific) to quantify *StFLORE* expression or by iScript cDNA synthesis kit to quantify *StCDF1*, *StCDF2* and *StCDF3*. The *NAC* gene was chosen as the housekeeping gene, and qRT-PCR was performed using SYBR green MasterMix (Bio-Rad, <https://www.bio-rad.com>) on a real-time PCR System (CFX96; Bio-Rad) with the specific primers listed in Table S4. The qRT-PCR programme consists of 95°C for 3 min and 42 cycles of 95°C for 5 sec and 60°C for 10 sec. The relative expression level of each examined gene was quantified by a relative quantification method.

ChIP-qPCR analysis

Chromatin immunoprecipitation (ChIP) on the *StCOs* cluster was performed as described elsewhere, with minor modifications (Abelenda *et al.*, 2016). We used a specific *StCDF1* antibody in a ChIP experiment on nuclear extracts from WT *S. andigena* plants and transgenic *S. andigena* overexpressing *StCDF1.2* from CaMV 35S promoter (*p35S:StCDF1.2*). A preliminary step of incubation and chromatin clean-up with the pre-immunized serum was included. After incubation with the antibody, chromatin isolation using G protein coupled to paramagnetic beads (Dynabeads Protein G; Novex Life Technologies, now ThermoFisher Scientific) was performed. After reverse crosslinking, chromatin was recovered by column purification using the QIAquick PCR clean up Kit (Qiagen, <https://www.qiagen.com>). ChIP-qPCR was assayed with specific primers to quantify *StCDF1* affinity for different *StCO1–StCO3* DNA binding sites, and the enrichment of eight separate amplified regions of the *StCO* gene cluster was quantified. Regarding *StCDF1* binding detection in the *StFLORE* promoter by ChIP, *SUC2:GFP-CDF1.1* transgenic plants in the CE3027 background were used. Plants were grown under LDs for 3 weeks, and material was collected at ZT4. Rabbit polyclonal anti-GFP antibody (Ab290; Abcam, <https://www.abcam.com>) was used in combination with Dynabeads Protein G and protein A (50/50 V/V). Control plants expressing GFP alone were used as a control. Four different regions were assayed by qPCR. Primer sequences are listed in Table S4. Regarding *StCDF1* binding detection in the *StFLORE* promoter by ChIP, *SUC2:GFP-CDF1.1* transgenic plants in the CE3027 background were used. Plants were grown under LDs for 3 weeks, and material was collected at ZT4. Rabbit polyclonal anti-GFP antibody (Ab290; Abcam) was used in combination with Dynabeads Protein G and protein A (50/50 V/V). Control plants expressing GFP alone were used as a control. Four different regions were assayed by qPCR. Primer sequences are listed in Table S4.

All ChIP enrichment calculations were performed using the SuperArray ChIP-qPCR Data Analysis Template (Qiagen/SABiosciences), following the manufacturer's instructions.

Protein binding microarray assay and analysis

Recombinant MBP-*StCDF1* protein was obtained in *E. coli* Rosetta™ strain (Novogen, <https://novogen-layers.com>) after cloning in pMAL-c2 vector (New England Biolabs, [\[neb.com\]\(https://www.neb.com\)\) using Gateway technology \(Figure S1a\). Proteins were purified according to the manufacturer's instructions. PBM-11 array design, incubation with transcription factors and binding affinity analysis are described elsewhere \(Abelenda *et al.*, 2016\).](https://www.</p>
</div>
<div data-bbox=)

Analysis of phenotypic data

Data analysis was performed using spss 22 (IBM, <https://www.ibm.com/analytics/spss-statistics-software>). Data obtained from the phenotypic variables evaluated were subjected to analysis of variance homogeneity to determine whether the distribution was normal. As the data presented a non-normal distribution, we applied a non-parametric test using the Kruskal–Wallis test. The differences among the genotypes were found through Fisher's least significant difference (LSD) test. The differences were considered significant for a value of $P \leq 0.05$.

ACKNOWLEDGEMENTS

The authors are grateful for the expertise of Dr Jan Schaart for approaches to design CRISPR-Cas9 mutagenesis. We also thank Ing. Dirk-Jan Huigen for expert assistance in the glasshouse and growth-room trials. We also acknowledge the kind support of Prof. Rossana Henriques for sharing her results prior to publication and for discussions of the results, and Dr Beatrix Horvath for helpful comments and a critical reading of the article. This work was supported by the ERA CAPS HotSol project funded by the Netherlands Organization for Scientific Research (NWO project 849.13.001), the FlowerPot project, supported by the Division for Earth and Life Sciences (ALW) with financial aid from the NWO. LRG received a fellowship from FONDECYT–CONCYTEC, Lima, Peru (grant no. 090-2016-FONDECYT). JAA was a recipient of an European Molecular Biology Organization (EMBO) fellowship (ASTF 485-2013) to perform the initial part of the research. JAA also wants to recognize the 'Severo Ochoa Program for Centres of excellence in R&D' from the State Research Agency (AEI; grant SEV-2016-0672), together with the Comunidad de Madrid Atracción de Talento Investigador programme (grant 2018T1/BIO11380) for their current financial support.

AUTHOR CONTRIBUTIONS

CWBB conceived and designed the experiments and wrote the article. JAA helped in the experimental design and in writing the article and producing the figures. LRG and LS carried out a large part of the experiments and helped in the assembly of the article and figures. SB helped conduct the experiments and supervised a part of the work. MO provided expert technical assistance. JMF-Z and RS-T carried out the protein binding microarray experiments and the analysis of the data. RGFV helped with overall supervision and critically edited the article.

CONFLICT OF INTEREST

The authors declare that they have no conflicts of interest for this work.

DATA AVAILABILITY STATEMENT

All relevant data can be found within the manuscript and its supporting materials.

SUPPORTING INFORMATION

Additional Supporting Information may be found in the online version of this article.

Figure S1. StCDF1 acts a repressor of StCO3.

Figure S2. StCDF1 knockdown non-redundantly delays tuberization.

Figure S3. The StCDF1 locus encodes for an antisense lncRNA called StFLORE.

Figure S4. StCDF1 knockdown shows enhanced drought tolerance.

Figure S5. Analysis of CRISPR/Cas9 pStFLORE plants and overexpressing StFLORE lines.

Figure S6. Analysis of CRISPR/Cas9 pStFLORE plants and overexpressing StFLORE lines.

Figure S7. Analysis of CRISPR/Cas9 pStFLORE plants and 35S:StFLORE lines.

Figure S8. Effect of StCDF1 expression on stomatal response to ABA treatment.

Figure S9. Effect of StFLORE expression on stomatal response to ABA treatment.

Table S1. Summary of the tuberization data of control (CE3027), StCDF1 RNAi and overexpressing StCDF1.2 independent lines.

Table S2. Summary of average stomatal features from StCDF1 RNAi, 35S:StCDF1, ΔpStFLORE, 35S:StFLORE and CE3027, as a control.

Table S3. List of plants from the C × E population used in this study.

Table S4. Oligonucleotides used in this study.

REFERENCES

- Abelenda, J.A., Cruz-Oro, E., Franco-Zorrilla, J.M. and Prat, S. (2016) Potato StCONSTANS-like1 suppresses storage organ formation by directly activating the FT-like StSP5G repressor. *Curr. Biol.* **26**, 872–881.
- Abelenda, J.A., Navarro, C. and Prat, S. (2014) Flowering and tuberization: a tale of two nightshades. *Trends Plant Sci.* **19**, 115–122.
- Aliche, E.B., Oortwijn, M., Theeuwens, T.P.J.M., Bachem, C.W.B., van Eck, H.J., Visser, R.G.F. and van der Linden, C.G. (2019) Genetic mapping of tuber size distribution and marketable tuber yield under drought stress in potatoes. *Euphytica*, **215**, 186.
- An, H., Roussot, C., Suarez-Lopez, P. et al. (2004) CONSTANS acts in the phloem to regulate a systemic signal that induces photoperiodic flowering of Arabidopsis. *Development*, **131**, 3615–3626.
- Andres, F. and Coupland, G. (2012) The genetic basis of flowering responses to seasonal cues. *Nat. Rev. Genet.* **13**, 627–639.
- Ariel, F., Romero-Barrios, N., Jégu, T., Benhamed, M. and Crespi, M. (2015) Battles and hijacks: noncoding transcription in plants. *Trends Plant Sci.* **20**, 362–371.
- Campo, S., Peris-Peris, C., Montesinos, L., Peñas, G., Messeguer, J. and San Segundo, B. (2012) Expression of the maize ZmGF14-6 gene in rice confers tolerance to drought stress while enhancing susceptibility to pathogen infection. *J. Exp. Bot.* **63**, 983–999.
- Corrales, A.R., Carrillo, L., Lasierra, P. et al. (2017) Multifaceted role of cycling DOF factor 3 (CDF3) in the regulation of flowering time and abiotic stress responses in Arabidopsis. *Plant Cell Environ.* **40**, 748–764.
- Corrales, A.R., Nebauer, S.G., Carrillo, L. et al. (2014) Characterization of tomato Cycling DoF Factors reveals conserved and new functions in the control of flowering time and abiotic stress responses. *J. Exp. Bot.* **65**(4), 995–1012.
- Cutler, J.M., Rains, D.W. and Loomis, R.S. (1977) The importance of cell size in the water relations of plants. *Physiol. Plant.* **40**, 255–260.
- Desikan, R., Hancock, J.T., Bright, J., Harrison, J., Weir, I., Hooley, R. and Neill, S.J. (2005) A role for ETR1 in hydrogen peroxide signaling in stomatal guard cells. *Plant Physiol.* **137**, 831–834.
- Eisele, J.F., Fäßler, F., Bürgel, P.F. and Chaban, C. (2016) A rapid and simple method for microscopy-based stomata analyses. *PLoS One*, **11**, e0164576.
- Fornara, F., de Montaigu, A., Sanchez-Villarreal, A., Takahashi, Y., Loren, V., van Themaat, E., Huettel, B., Davis, S.J. and Coupland, G. (2015) The Gl-CDF module of Arabidopsis affects freezing tolerance and growth as well as flowering. *Plant J.* **81**, 695–706.
- Fornara, F., Panigrahi, K.C., Gissot, L., Sauerbrunn, N., Ruhl, M., Jarillo, J.A. and Coupland, G. (2009) Arabidopsis DOF transcription factors act redundantly to reduce CONSTANS expression and are essential for a photoperiodic flowering response. *Dev. Cell*, **17**, 75–86.
- Franco-Zorrilla, J.M., Lopez-Vidriero, I., Carrasco, J.L., Godoy, M., Vera, P. and Solano, R. (2014) DNA-binding specificities of plant transcription factors and their potential to define target genes. *Proc. Natl. Acad. Sci. USA*, **111**, 2367–2372.
- Godoy, M., Franco-Zorrilla, J.M., Perez-Perez, J., Oliveros, J.C., Lorenzo, O. and Solano, R. (2011) Improved protein-binding microarrays for the identification of DNA-binding specificities of transcription factors. *Plant J.* **66**, 700–711.
- Gutaker, R.M., Weiss, C.L., Ellis, D., Anglin, N.L., Knapp, S., Luis Fernandez-Alonso, J., Prat, S. and Burbano, H.A. (2019) The origins and adaptation of European potatoes reconstructed from historical genomes. *Nat. Ecol. Evol.* **3**, 1093–1101.
- Henriques, R., Wang, H., Liu, J., Boix, M., Huang, L.F. and Chua, N.H. (2017) The antiphase regulatory module comprising CDF5 and its antisense RNA FLORE links the circadian clock to photoperiodic flowering. *New Phytol.* **216**, 854–867.
- Imaizumi, T. and Kay, S.A. (2006) Photoperiodic control of flowering: not only by coincidence. *Trends Plant Sci.* **11**, 550–558.
- Imaizumi, T., Schultz, T.F., Harmon, F.G., Ho, L.A. and Kay, S.A. (2005) FKF1 F-box protein mediates cyclic degradation of a repressor of CONSTANS in Arabidopsis. *Science*, **309**, 293–297.
- Jefferson, R.A., Kavanagh, T.A. and Bevan, M.W. (1987) GUS fusions: beta-glucuronidase as a sensitive and versatile gene fusion marker in higher plants. *EMBO J.* **6**, 3901–3907.
- Karimi, M., Inze, D. and Depicker, A. (2002) GATEWAY(TM) vectors for Agrobacterium-mediated plant transformation. *Trends Plant Sci.* **7**, 193–195.
- Kloosterman, B., Abelenda, J.A., Gomez, M.D.C. et al. (2013) Naturally occurring allele diversity allows potato cultivation in northern latitudes. *Nature*, **495**, 246–250.
- Kondhare, K.R., Vetal, P.V., Kalsi, H.S. and Banerjee, A.K. (2019) BEL1-like protein (StBEL5) regulates CYCLING DOF FACTOR1 (StCDF1) through tandem TGAC core motifs in potato. *J. Plant Physiol.* **241**, 153014.
- Matsui, A. and Seki, M. (2019) The involvement of long noncoding RNAs in response to plant stress. *Methods Mol. Biol.* **1933**, 151–171.
- McCree, K.J. and Davis, S.D. (1974) Effect of water stress and temperature on leaf size and on size and number of epidermal cells in Grain Sorghum 1. *Crop Sci.* **14**, 751–755.
- Murashige, T. and Skoog, F. (1962) A revised medium for rapid growth and bio assays with tobacco tissue cultures. *Physiol. Plant.* **15**, 473–497.
- PGSC; Potato Genome Sequencing Consortium. (2011) Genome sequence and analysis of the tuber crop potato. *Nature*, **475**, 189–195.
- Plesch, G., Ehrhardt, T. and Mueller-Roeber, B. (2001) Involvement of TAAAG elements suggests a role for DoF transcription factors in guard cell-specific gene expression. *Plant J.* **28**, 455–464.
- Quarrie, S.A. and Jones, H.G. (1977) Effects of abscisic acid and water stress on development and morphology of wheat. *J. Exp. Bot.* **28**, 192–203.
- Renau-Morata, B., Molina, R.V., Carrillo, L. et al. (2017) Ectopic expression of CDF3 genes in tomato enhances biomass production and yield under salinity stress conditions. *Front. Plant Sci.* **8**, 660.
- Roelfsema, M.R.G. and Prins, H.B.A. (1995) Effect of abscisic acid on stomatal opening in isolated epidermal strips of abi mutants of Arabidopsis thaliana. *Physiol. Plant.* **95**, 373–378.
- Sawa, M., Nusinow, D.A., Kay, S.A. and Imaizumi, T. (2007) FKF1 and GIGANTEA complex formation is required for day-length measurement in Arabidopsis. *Science*, **318**, 261–265.

- Sharma, P., Lin, T. and Hannapel, D.J.** (2016) Targets of the StBEL5 transcription factor include the FT ortholog StSP6A. *Plant Physiol.* **179**, 310–324.
- Song, Y.H., Smith, R.W., To, B.J., Millar, A.J. and Imaizumi, T.** (2012) FKF1 conveys timing information for CONSTANS stabilization in photoperiodic flowering. *Science*, **336**, 1045–1049.
- Spence, R.D.** (1987) The problem of variability in stomatal responses, particularly aperture variance, to environmental and experimental conditions. *New Phytol.* **107**, 303–315.
- Spitters, C.J.T. and Schapendonk, A.** (1990) Evaluation of breeding strategies for drought tolerance in potato by means of crop growth simulation. *Plant and Soil*, **123**, 151–161.
- Spooner, D.M., Nunez, J., Trujillo, G., Herrera Mdel, R., Guzman, F. and Ghislain, M.** (2007) Extensive simple sequence repeat genotyping of potato landraces supports a major reevaluation of their gene pool structure and classification. *Proc. Natl. Acad. Sci. USA*, **104**, 19398–19403.
- Wu, Q., Liu, X., Yin, D., Yuan, H., Xie, Q., Zhao, X., Li, X., Zhu, L., Li, S. and Li, D.** (2017) Constitutive expression of OsDof4, encoding a C2–C2 zinc finger transcription factor, confers its distinct flowering effects under long- and short-day photoperiods in rice (*Oryza sativa* L.). *BMC Plant Biol.* **17**, 166.
- Yanagisawa, S. and Schmidt, R.J.** (1999) Diversity and similarity among recognition sequences of Dof transcription factors. *Plant J.* **17**, 209–214.
- Yang, H. and Wang, G.** (2001) Leaf stomatal densities and distribution in *triticum aestivum* under drought and CO₂ enrichment. *Acta Phytoecol. Sin.* **25**, 312–316.
- Yang, L., Mei, H., Guangsheng, Z. and Jiandong, L.** (2007) The changes in water-use efficiency and stoma density of *Leymus chinensis* along Northeast China Transect. *Acta Ecol. Sin.* **27**, 16–23.
- Zhang, Y., Wang, Z. and Wu, Y.** (2006) Stomatal characteristics of different green organs in wheat under different irrigation regimes. *Acta Agron. Sin.* **32**, 70–75.